Preparation of ZnS by magnetron sputtering and its buffer effect on the preferential orientation growth of ITO thin film

Wenhan Du[1,2] ✉, *Jingjing Yang*[1], *Yu Zhao*[1], *Chao Xiong*[1]

[1]*School of Electrical and Photoelectronic Engineering, Changzhou Institute of Technology, #666, Liaohe Road, Changzhou, Jiangsu, 213002, People's Republic of China*
[2]*School of Materials Science and Engineering, Nanyang Technological University, Block N4.1, Nanyang Avenue, 639798, Singapore*
✉ *E-mail: duwenhan@ntu.edu.sg*

Published in Micro & Nano Letters; Received on 5th September 2017; Revised on 11th November 2017; Accepted on 2nd January 2018

Two different deposition sequences were carried to investigate ZnS and indium-tin oxide (ITO) multiple thin films on quartz substrates using magnetron sputtering technique. In the deposition order of ITO on ZnS layer, ZnS acts as a buffer layer with a thickness of at least 10 nm, and ITO thin film has (222) preferential orientation growth. Besides, lattice constant expansion phenomenon was observed when the film thickness of ITO was increased, indicating tension stress increase in ITO film. The lattice constant mismatch of 5% is the reason for the preferential orientation growth between ZnS and ITO thin films. In the other deposition sequence of ZnS on ITO layer, ZnS thin film has (111) preferential orientation growth. While ITO was kept in multiple crystalline properties. Pinhole-free ZnS thin film was observed by scanning electron microscopy for this deposition sequential, promising well interface in the thin film solar cells with lower interface defects.

1. Introduction: Indium-tin oxide (ITO) thin films are technically important functional oxide materials which are widely used in thin-film solar cells, transparent electronics and LED devices. In recent years, the deposition of ITO thin films on flexible substrates has attracted many interests since the multiple applications of flexible solar cells, where ITO thin films can be used as electrodes to collect the electrons generated from the absorption layers [1–10]. The crystalline structure and quality of ITO thin films have a significant influence on the device properties.

ZnS is an n-type wide energy bandgap semiconductor with an E_g value of 3.7–4.1 eV. ZnS, therefore, allows more photons to enter into the absorption layers than the traditional n-type semiconductor CdS, thus increase photocurrent [11–21]. ZnS is thus considered as a possible partner material to form p–n junctions in thin-film solar cells such as CdTe and CIGS [22–24].

In the substrate configuration of CdTe and CIGS solar cells, ITO was deposited on the ZnS layer, while in the superstrate configuration ZnS was deposited on the ITO layer. In order to explore the influence of ZnS on the structure and morphology of the ITO thin films, we used quartz glass as the substrate, and two different deposition sequences were used, one was ITO on the ZnS layer, the other was ZnS on the ITO layer. We found that the ITO thin film had a preferential orientation growth with the assistance of the ZnS buffer layer, while in the other deposition order of ZnS on ITO, pinhole-free thin film was obtained.

2. Experiment: ITO and ZnS thin films were deposited by the magnetron sputtering technique [25]. Both sputtering targets were hot-pressed ceramics, and quartz glasses were used as the substrates. Both radio frequency (RF) and DC powers were supplied by AE Company (USA). The size of quartz glass substrates was 1×1 cm^2, ultrasonically cleaned in acetone, isopropyl alcohol and deionised water, and then blown with 5N N_2 gas. The substrates were then put into the vacuum chamber. Before the film deposition, the chamber vacuum pressure was pumped to 2.0×10^{-4} Pa. High-purity Ar gas was then fed into the chamber until the vacuum pressure reached 7 Pa, this was the better point to ignite the plasma in the chamber.

ZnS buffer layer preparation: The ZnS target was pre-sputtered 5 min to remove any possible contamination. Then, the ZnS thin film was deposited onto the quartz substrate under an RF power of 70 W, a vacuum pressure of 2.0 Pa, a substrate temperature of 180°C, and the deposition time changed from 1 to 50 min.

ITO thin-film preparation: the ITO thin film was deposited onto the ZnS/quartz substrate. During deposition, the vacuum pressure was kept at 1.0 Pa, the DC power was changed between 70 and 130 W, the substrate temperature was kept at 180°C, and the deposition time was changed from 1 to 60 min. The thickness of ITO thin film was measured by cross-section scanning electron microscopy (SEM) image and calibrated using a surface profiler.

The structural information of the films was analysed using X-ray diffraction (XRD) measurement (Rigaku, Ultima IV) with CuKα ($\lambda = 1.54060$ Å). The XRD data were collected in the 2θ range from 20° to 70° with a step of 0.02°. The morphology information of the films was analysed by field emission SEM (Zeiss, Sigma). The element components of the oxidation films were collected by energy dispersive X-ray spectroscopy (EDS, Oxford) which installed in SEM chamber.

3. Results and discussion: Before investigating the influence of ZnS on the growth of the ITO thin film and vice versa, ZnS and ITO single layers on the quartz substrates were prepared separately. The XRD results of single layer ITO, ZnS, and ITO on ZnS are shown in Fig. 1. Fig. 1*a* shows the XRD pattern of the ITO single layer. Four main peaks, corresponding to (222), (400), (440), and (622), appearing in the 2θ range between 25° and 70°, indicating the multiple crystalline properties of the ITO single layer thin films on the quartz substrate. This result was similar to the report of Zheng *et al.* [6]. Fig. 1*b* shows the XRD pattern of the ZnS single layer. Only one prominent diffraction peak, with a peak position of 28.78°, corresponding to the (111) crystalline face, is observed in the diffraction diagram. This indicates that the growth of the ZnS thin film on the quartz substrate had a preferential orientation with a zinc blende structure, similar to the result reported in [11, 12]. Fig. 1*c* shows the influence of the ZnS buffer layer (80 nm) on the growth of the ITO thin film (250 nm). There is one prominent ITO (222) diffraction peak; the other diffraction peaks are very weak. This indicates that with the addition of the ZnS buffer layer, the ITO film exhibits preferential orientation

© The Institution of Engineering and Technology 2018

doi: 10.1049/mnl.2017.0647

growth. And the crystalline size was ~37 nm of ITO (222) as calculated using the Scherrer equation.

In order to investigate the influence of sputtering power on the structure of ITO thin film with ZnS buffer layers, we prepared a series samples with different thickness, the XRD results are shown in Fig. 2*a*. The diffraction peak position of ITO (222) of three samples has prominent shift, which is 30.547°, 30.289°, and 30.201° as the film thickness is increased from 110 to 200 nm, and the total diffraction angle shift was 0.34°. This indicates that with the thickness increase the lattice constant of ITO (222) crystalline face is increased from 0.292398 to 0.295068 nm, which expands about 0.913%. The lattice constant expansion phenomenon indicates tension stress increase in ITO film as film thickness increase.

In order to investigate the influence of ZnS thickness on ITO layer, a series samples with a different thickness of ZnS layer were prepared, the minimum was 2 nm and the maximum was 40 nm, and kept all the ITO thickness at 110 nm. The XRD results are shown in Fig. 2*b*. From this diagram, the minimum effective thickness of ZnS is about 10 nm, as the peak height is increased prominently. This can be explained as the coverage changes for different ZnS thickness, the minimum thickness required for cover the substrate is about 10 nm.

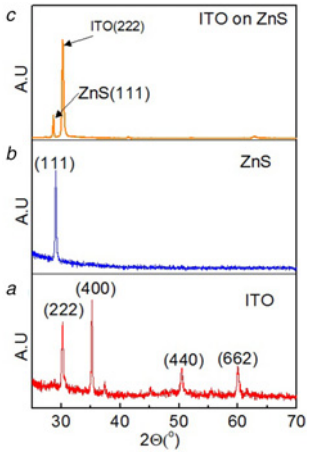

Fig. 1 *XRD results of*
a Single-layer ITO thin film (180 nm) on quartz
b Single layer ZnS (80 nm) on quartz substrates
c XRD patterns of (222) preferential orientation of ITO film (250 nm) on ZnS buffer layer (80 nm)

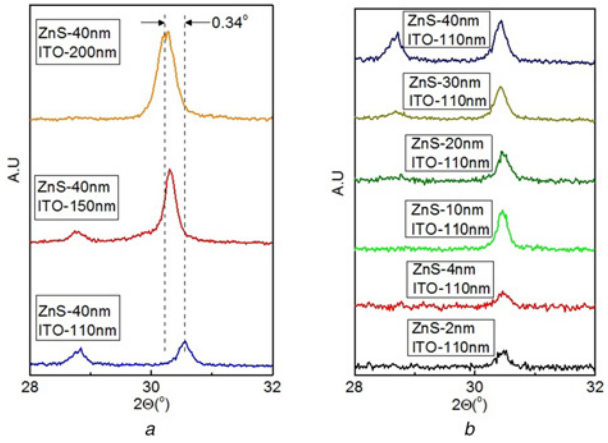

Fig. 2 *Thickness influence of ZnS buffer layer and ITO thin films*
a Thickness dependent of ITO (222) peak position with ZnS buffer layer, the thickness of ITO was 110, 150, and 200 nm from bottom to up, and the ZnS thickness was kept at 40 nm
b Thickness influence of ZnS on ITO (222) peak height, ITO thickness was fixed at 110 nm, and the thickness of ZnS was an increase from 2 to 40 nm

The SEM results of the ZnS-buffered ITO thin film are shown in Fig. 3. The average crystalline size of ITO thin films is about 40 nm from high resolution SEM image in Fig. 3*b*. This was similar to the results calculated from the XRD pattern. Clear grain boundaries can be seen in this image, indicating better crystalline quality using ZnS buffer layer.

When replacing CdS with ZnS in the thin film solar cell, if adopt superstrate structure, ZnS will deposit on front contact such as ITO thin film [22–24]. ZnS/ITO complex film was prepared using magnetron sputtering and the structural and morphology information were investigated. Fig. 4 shows the XRD result of ZnS growth on ITO layer, ZnS thin film has preferential orientation growth and ITO has multiple crystalline structures. SEM result indicates large changes in morphology of this sequence multiple layers, as shown in Fig. 5. ZnS film is quite dense, and there has no any pinholes in the large area SEM image as shown in

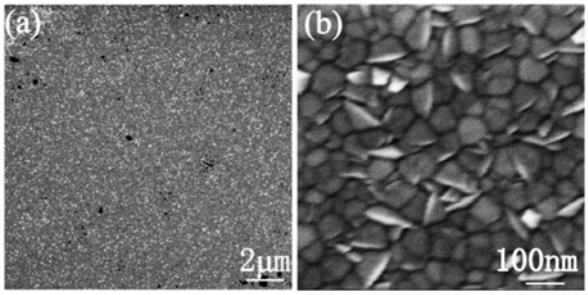

Fig. 3 *SEM images of ZnS-buffered ITO thin film*
a Large-scale SEM image
b Magnified SEM image of ZnS-buffered ITO thin film, the thickness of ZnS and ITO was 80 and 250 nm separately

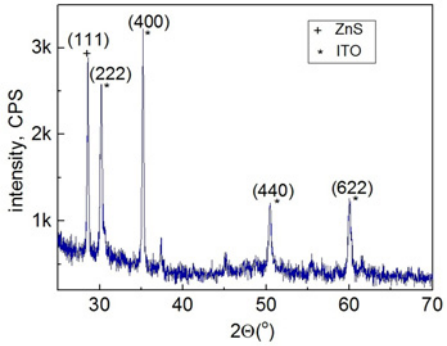

Fig. 4 *XRD result of ZnS deposited on ITO layers, ZnS and ITO thicknesses were 80 and 180 nm separately*

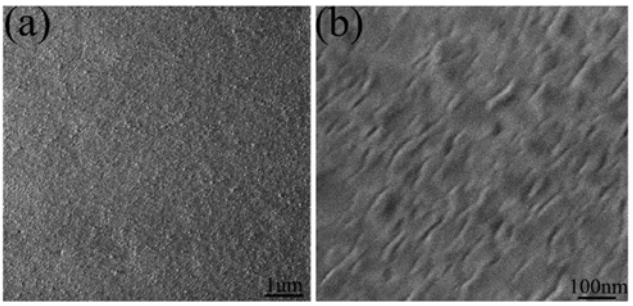

Fig. 5 *SEM images of ZnS on ITO thin films*
a Large-scale SEM image
b Magnified SEM image of ZnS thin film with a thickness of 160 nm. The under layer was ITO thin film with thickness of 120 nm

© The Institution of Engineering and Technology 2018

Fig. 5*a*, while compared with Fig. 3*a* there exist several pinholes in the ZnS buffered ITO thin films. This pinhole-free ZnS thin film will facility the good interface during form pn junction with p-type semiconductor in the fabrication of thin film solar cells.

ZnS exhibited preferential orientation growth on the quartz substrate as suggest from Fig. 1*b*. The lattice constant of ZnS (111) crystalline face is 0.31151 nm, whereas the lattice constant of ITO (222) crystalline face is 0.29566 nm. Thus, the lattice constant mismatch of these two layers is ∼5%. If the lattice constant mismatch is smaller than 5% in the hetero-layer, epitaxial growth may be obtained, such as the epitaxial growth of $SrTiO_3$ on Si substrate [26–28]. Therefore, the reason for the ITO preferential orientation growth on the ZnS buffer layer is the small lattice constant mismatch. Another case can be found in the preferential orientation growth of ITO thin film with the ZnO buffer layer reported by Sun and Du [9, 29, 30], since ZnS and ZnO have the same crystalline structure.

4. Conclusion: Two different deposition sequences were used to investigate ZnS and ITO double layer thin films. In the deposition sequence of ITO on ZnS layer, ZnS behave as a buffer layer, the ITO thin film will have preferential orientation growth with (222) crystalline face. The minimum thickness of ZnS was 10 nm in this case. Besides, there has lattice constant expansion phenomenon when the film thickness of ITO was increased, indicating tension stress increase in ITO film. The lattice constant mismatch of 5% is the reason for the preferential orientation between ZnS and ITO thin films. In the other deposition sequence of ZnS on ITO layer, ZnS thin film will have preferential orientation growth with (111) crystalline face. While ITO was kept in multiple crystalline property. Pinhole free ZnS thin film was observed by SEM for this deposition sequence, promising well interface in the thin film solar cells with lower interface defects.

5. Acknowledgments: This work was supported by National Nature Science foundation of China grant no. 61540071, Project of Jiangsu Natural Science Research of High Education grant no. 15KJD140002, Fundamental Research Funds of Changzhou Science and Technology Bureau grant no. CJ20160026, Natural Science Funds of Changzhou Institute of Technology grant no. YN1408. The Top-notch Academic Programs Project of Jiangsu Higher Education Institutions (TAPP) with grant no. PPZY2015B129.

6 References

[1] Kim S., Lee K., Sahu B., *ET AL.*: 'Flexible OLED fabrication with ITO thin film on polymer substrate', *Jap. J. Appl. Phys.*, 2015, **54**, p. 090301

[2] Gwamuri J., Vora A., Mayandi J., *ET AL.*: 'A new method of preparing highly conductive ultra-thin indium tin oxide for plasmonic-enhanced thin film solar photovoltaic devices', *Sol. Energy Mater. Sol. Cells*, 2016, **149**, pp. 250–257

[3] Saklayen G., Islam S., Rahman F., *ET AL.*: 'Investigation on the effect of film thickness on the surface morphology, electrical and optical properties of E-beam deposited indium tin oxide (ITO) thin film', *Adv. Mat. Phys. Chem.*, 2014, **4**, pp. 194–202

[4] Rana R., Chakraborty J., Tripathi S.K., *ET AL.*: 'Study of conducting ITO thin film deposition on flexible polyimide substrate using spray pyrolysis', *J. Nanostructure Chem.*, 2016, **6**, (1), pp. 65–74

[5] Meng L., Teixeira V., Santos M.: 'Characteristics of ion beam assisted ITO thin films deposited by RF magnetron sputtering', *Phys. Status Solidi A*, 2010, **207**, pp. 1538–1542

[6] Zheng H.J., Zhang C., Ruan Z.: 'Optimization in synthesis of ITO thin films fabricated by DC magnetron sputtering method', *Appl. Mech. Mater.*, 2014, **575**, pp. 254–263

[7] Nisha M., Anusha S., Antony A., *ET AL.*: 'Effect of substrate temperature on the growth of ITO thin films', *Appl. Surf. Sci.*, 2005, **252**, (5), pp. 1430–1435

[8] Terzini E., Thilakan P., Minarini C.: 'Properties of ITO thin films deposited by RF magnetron sputtering at elevated substrate temperature', *Mater. Sci. Eng. B*, 2000, **77**, (1), pp. 110–114

[9] Herrero J., Guillén C.: 'Improved ITO thin films for photovoltaic applications with a thin ZnO layer by sputtering', *Thin Solid Films*, 2004, **451–452**, pp. 630–633

[10] Han G.F., Zhang S., Boix P.P., *ET AL.*: 'Towards high efficiency thin film solar cells', *Prog. Mater. Sci.*, 2017, **87**, pp. 246–291

[11] Chelvanathan P., Yusoff Y., Haque F., *ET AL.*: 'Growth and characterization of RF-sputtered ZnS thin film deposited at various substrate temperatures for photovoltaic application', *Appl. Surf. Sci.*, 2015, **334**, pp. 138–144

[12] Özkan M., Ekem N., Pat S., *ET AL.*: 'Zns thin film deposition on silicon and glass substrates by thermionic vacuum Arc', *Mater. Sci. Semicon. Proc.*, 2012, **15**, pp. 113–119

[13] Ghribi F., El Mira L., Omri K., *ET AL.*: 'Sputtered ZnS thin film from nanoparticles synthesized by hydrothermal route', *Optik*, 2016, **127**, pp. 3688–3692

[14] Qiu K.F., Qiu D.P., Cai L., *ET AL.*: 'Preparation of ZnS thin films and ZnS/p-Si heterojunction solar cells', *Mater. Lett.*, 2017, **198**, pp. 23–26

[15] Kong L., Deng J., Chen L.: 'Structural and optical characterization of magnetron sputtered ZnS thin films annealed in different atmosphere', *Chalcogenide Lett.*, 2017, **14**, (3), pp. 87–96

[16] Kim D.R., Hwang D.Y., Son C.S., *ET AL.*: 'Effect of sputtering power on the structure and optical properties of radio frequency sputtered-ZnS thin film', *J. Nanosci. Nanotechnol.*, 2017, **17**, pp. 5046–5049

[17] Hwang D.Y., Son C.S.: 'Characterization of RF sputtered-ZnS thin film grown at various annealing temperatures', *J. Nanosci. Nanotechnol.*, 2017, **17**, pp. 5042–5045

[18] Liang G., Fan P., Chen C.: 'Improved microstructure and properties of CBD-ZnS thin films', *J. Mater. Sci. Mater. Electron.*, 2015, **26**, p. 2230

[19] Kurnia F., Yun H.N., Tang Y.M., *ET AL.*: 'ZnS thin films for visible-light active photoelectrodes: effect of film morphology and crystal structure', *Cryst. Growth Des.*, 2016, **16**, (5), pp. 2461–2465

[20] Goudarzi A., Namghi A.D., Ha C.S.: 'Fabrication and characterization of nano-structured ZnS thin films as the buffer layers in solar cells', *RSC Adv.*, 2014, **4**, pp. 59764–59771

[21] Liu J., Wei A.X., Zhao Y.: 'Effect of different complexing agents on the properties of chemical-bath-deposited ZnS thin films', *J. Alloy. Compd.*, 2014, **588**, pp. 228–234

[22] Kim J., Park C., Pawar S.M., *ET AL.*: 'Optimization of sputtered ZnS buffer for Cu_2ZnSnS_4 thin film solar cells', *Thin Solid Films*, 2014, **566**, pp. 88–92

[23] Lim D.G., Park J.E., Lee S.H., *ET AL.*: 'The effect of ZnS buffer layer added sodium citrate on copper indium gallium selenide thin film solar cells', *J. Nanosci. Nanotechnol.*, 2017, **17**, pp. 3514–3518(5)

[24] Li W., Chen J., Yan C., *ET AL.*: 'The effect of ZnS segregation on Zn-rich CZTS thin film solar cells', *J. Alloys Compd.*, 2015, **632**, pp. 178–184

[25] Du W.H., Yang J.J., Zhao Y., *ET AL.*: 'Effects of Mg doping content and annealing temperature on the structural properties of $Zn_{1-x}Mg_xO$ thin films prepared by radio-frequency magnetron sputtering', *Optoelectro. Lett.*, 2017, **13**, pp. 42–44

[26] Hu X.M., Li H., Liang Y., *ET AL.*: 'The interface of epitaxial $SrTiO_3$ on silicon: in situ and ex situ studies', *Appl. Phys. Lett.*, 2003, **82**, p. 203

[27] Wu H.W., Aoki T., Agham B.P., *ET AL.*: 'Anti-phase boundaries at the $SrTiO_3$/Si(001) interface studied using aberration-corrected scanning transmission electron microscopy', *Appl. Phys. Lett.*, 2016, **108**, p. 091605

[28] Guillaume S.G., Bachelet R., Moalla R., *ET AL.*: 'Epitaxy of $SrTiO_3$ on silicon: the knitting machine strategy', *Chem. Mater.*, 2016, **28**, (15), pp. 5347–5355

[29] Sun X.W., Wang L.D., Kwok H.S.: 'Improved ITO thin films with a thin ZnO buffer layer by sputtering', *Thin Solid Films*, 2000, **360**, pp. 75–81

[30] Du W.H., Yang J.J., Xiong C., *ET AL.*: 'Preferential orientation growth of ITO thin film on quartz substrate with ZnO buffer layer by magnetron sputtering technique', *Int. J. Mod. Phys. B*, 2017, **31**, p. 1744065

© The Institution of Engineering and Technology 2018

doi: 10.1049/mnl.2017.0647